Kosambi-Cartan-Chern Analysis of the Nonequilibrium Singular Point in One-Dimensional Elementary Catastrophe

Yamasaki, Kazuhito

Yajima, Takahiro

(Citation)
International Journal of Bifurcation and Chaos,32(04):2250053

(Issue Date)
2022-03-30

(Resource Type)
journal article

(Version)
Accepted Manuscript

International Journal of Bifurcation and Chaos

Kosambi-Cartan-Chern analysis of the non-equilibrium singular point in one-dimensional elementary catastrophe

Kazuhito Yamasaki
Department of Planetology, Graduate School of Science, Kobe University, Nada, Kobe 657-8501, Japan
yk2000@kobe-u.ac.jp

Takahiro Yajima
Department of Mechanical Systems Engineering, Faculty of Engineering, Utsunomiya University, Utsunomiya, 321-8585, Japan
yajima@cc.utsunomiya-u.ac.jp

Received (to be inserted by publisher)

This paper analyzes the properties of the non-equilibrium singular point in one-dimensional elementary catastrophe. For this analysis, the Kosambi-Cartan-Chern (KCC) theory is applied to characterize the dynamical system based on differential geometrical quantities. When both the nonlinear connection and deviation curvature are zero, that is, when the geometric stability of the KCC theory is neutral, two bifurcation curves are obtained: one is the known curve with an equilibrium singular point, and the other is a new curve with a non-equilibrium singular point. The two singular points are distinguished based on the vanishing condition of the Berwald connection. Applied to the ecosystem described by the Hill function, the absolute value of the cuspidal curvature of the non-equilibrium singular point is larger than that of the equilibrium singular point. The ecological interpretation of this result is that the range of bistability of the ecosystem in the non-equilibrium state is greater than that in the equilibrium state. The type of singular points in equilibrium and non-equilibrium bifurcation curves are not necessarily the same. For instance, there is a combination in which even if the former has one cusp, the latter may show various types, depending on the parametric space. These results demonstrate that there are cases where simply shifting the system from the equilibrium to non-equilibrium state expands the range of bistability and changes the type of singularity. Although singularity analysis is often performed near the equilibrium point, non-equilibrium analysis, i.e., analysis based on the KCC theory, provides a useful perspective for analyzing singularity theory according to the bifurcation phenomenon.

Keywords: singular point; KCC theory; bifurcation theory; non-equilibrium; elementary catastrophe; differential geometry

1. Introduction

The Kosambi-Cartan-Chern (KCC) theory can be used to characterize systems from the properties of ordinary differential equations, such as bifurcation and stability, based on differential geometric quantities (e.g., [Antonelli *et al.*, 1993; Yamasaki & Yajima, 2017; Gupta, & Yadav, 2019; Huang *et al.*, 2019; Chen *et al.*, 2020]). KCC theory has been well studied in the field of differential geometry, especially Finsler geometry [Antonelli & Bucataru, 2001; Balan & Neagu, 2010; Neagu, 2013], and it has been applied to various fields

such as biology [Antonelli *et al.*, 2002] and physics [Boehmer & Harko, 2010; Harko & Sabău, 2008; Harko *et al.*, 2015; Dănilă *et al.*, 2016; Gupta & Yadav, 2017], among others [Liu *et al.*, 2021]. For instance, Yamasaki and Yajima (2020) performed KCC analysis of bifurcation phenomena including catastrophe. Given that catastrophe is closely related to the singularity of the system [Thom, 1972; Zeeman, 1977; Gilmore, 1981; Arnol'd, 2003; Izumiya *et al.*, 2016], this implies that the KCC and singularity theories are related through bifurcation phenomena. The main focus of catastrophe theory is, of course, the catastrophe shift exhibited by singularities, which are in a non-equilibrium state during the shift. Therefore, non-equilibrium stability analysis of the various shifts exhibited by singularities is necessary, but not sufficient. KCC theory has shown utility for non-equilibrium stability analysis. Thus, we performed KCC analysis of the basic singularities of catastrophe theory and analyzed their behavior in the non-equilibrium region.

The logistic equation with the Hill function is a typical example of a catastrophe in ecology [Ludwig *et al.*, 1978; Scheffer et al., 2009; Strogatz, 2014]. Applying the KCC theory to this equation, we can derive the differential geometric quantities governing the stability of the system: nonlinear connection N^i_j and deviation curvature P^i_j. When both N^i_j and P^i_j are zero, i.e., the geometrical stability becomes neutral, we can obtain two bifurcation curves with a singular point [Yamasaki & Yajima, 2020]. (Their concrete forms are described by Eqs. (36) and (37) in Section 3.) The first is a known bifurcation curve with a singular point; however, the second curve with a singular point has not been fully analyzed. The main purpose of this study is to clarify the reason for the two types of singular points: the well-known equilibrium singular point and the lesser-known non-equilibrium singular point. Catastrophe theory is mainly concerned with singularities at equilibrium. However, as mentioned above, the catastrophe shift contains a non-equilibrium state. Here, we examine whether non-equilibrium singularities exist and their properties. The results are expected to provide a new perspective on singular points in relation to bifurcations. To quantitatively show the difference between equilibrium and non-equilibrium singularities, this study introduces the concept of curvature at a singularity. Calculations at singularities almost always fail; however, recent research has made it possible to calculate the curvature of singularities [Saji *et al.*, 2010; Umehara, 2011]. Comparing the curvature among singularities will reveal a case in which the range of bistable states increases by simply shifting the system from an equilibrium to non-equilibrium state.

From the viewpoint of catastrophe theory, there are various types of singular points [Thom, 1972; Arnol'd, 2003; Izumiya *et al.*, 2016]. In the case of the Hill function given above, we see that the singular points in the equilibrium and non-equilibrium states are of the same type, i.e., that of a cusp. However, this does not always hold. Here, we also consider the difference in the types of singular points between the two states based on well-known singular points in elementary catastrophe theory: cusp, swallowtail, and butterfly. This analysis will show, for instance, that there are combinations in which the equilibrium singular point is the cusp, but the non-equilibrium singular point is the swallowtail. This result indicates that the type of singularity changes when the system shifts from an equilibrium to non-equilibrium state, even if the control parameters do not change. Such non-equilibrium analysis will be possible by focusing on the basic geometric quantities in KCC theory, especially the deviation curvature and Berwald connection.

The structure of this paper is as follows. In Section 2, we provide a brief review of KCC theory in terms of time-like potential, and apply it to the normal form of elementary catastrophe as an example. In this example, there is one bifurcation curve with a singular point. In Section 3, we consider the logistic equation with the Hill function and show that there are two types of singular points: equilibrium and non-equilibrium ones. This result indicates the geometrical conditions necessary for the existence of non-equilibrium singularities. This condition is applied to the elementary catastrophe considered in Section 4, to show the existence and difference in non-equilibrium singular points among various parametric spaces. Section 5 provides our conclusions.

2. A brief review of KCC theory

2.1. *Differential geometrical quantities and stability*

The KCC theory was first applied to study the geometric invariance of second-order ordinary differential equations (ODEs) [Kosambi, 1933; Cartan, 1933; Chern, 1939; Antonelli *et al.*, 1993]. Since then, KCC theory has been applied to study the stability of dynamical systems (e.g., [Antonelli *et al.*, 1993; Udriste &

Nicola, 2009; Abolghasem, 2013; Yamasaki & Yajima, 2013]). Even more recently, numerous studies have investigated the geometric aspects of various dynamic structures, including those of physical (e.g., [Kumar *et al.*, 2019; Krylova *et al.*, 2019; Alawadi *et al.*, 2020; Liu *et al.*, 2020; Klën, & Molina, 2020; Wang *et al.*, 2021]), biological (e.g., [Antonelli *et al.*, 2014; Antonalli *et al.*, 2019; Kolebaja, & Popoola, 2019; Mishra, & Tiwari, 2021]), and general (e.g., [Gupta, & Yadav, 2017; Sulimov *et al.*, 2018; Chen, & Yin, 2019; Feng *et al.*, 2020; Salnikova *et al.*, 2020; Liu *et al.*, 2021]) systems.

Let us consider the second-order ODE:

$$\ddot{x}^i + g^i(x, \dot{x}) = 0, \tag{1}$$

where $g^i(x, \dot{x})$ is a function. According to KCC theory, a small perturbation in the trajectory of (1) gives the covariant form of the variational equation (e.g., [Antonelli, & Bucataru, 2003]):

$$\frac{D^2 u^i}{Dt^2} = P^i_j u^j, \tag{2}$$

where $D(\cdots)/Dt$ is a covariant differential, and the initial conditions are given by $u(0) = 0$ and $\dot{u}(0) \neq 0$. P^i_j is the geometric object or deviation curvature tensor, defined by the following relation:

$$P^i_j = -\frac{\partial g^i}{\partial x^j} + \frac{\partial N^i_j}{\partial x^k}\dot{x}^k - G^i_{jk} g^k + N^i_k N^k_j, \tag{3}$$

where N^i_j is a nonlinear connection:

$$N^i_j = \frac{1}{2}\frac{\partial g^i}{\partial \dot{x}^j}, \tag{4}$$

and G^i_{jk} is a Berwald connection:

$$G^i_{jk} = \frac{\partial N^i_j}{\partial \dot{x}^k}. \tag{5}$$

From the Berwald connection, the Douglas tensor is defined by $D^i_{jkl} = \partial G^i_{jk}/\partial \dot{x}^l$. Because this paper considers the one-dimensional case, we set $x^1 = x$, $g^1 = g$, $G^1_{11} = G$, $N^1_1 = N$, $P^1_{11} = P$, and $D^1_{11} = D$ for simplicity.

The deviation curvature (3) determines the Jacobi stability of the system, i.e., the robustness of its trajectory[Sabău, 2005a; Harko *et al.*, 2016; Lake & Harko, 2016]. The trajectory of a one-dimensional system is Jacobi-stable when P is negative, and Jacobi-unstable when P is positive [Antonelli, & Bucataru, 2003; Sabău, 2005a,b]. For convenience, we refer to the system as being J-stable when $P < 0$, as J-unstable when $P > 0$, and as J-neutral when $P = 0$. Moreover, we consider the nonlinear connection (4), as this is also related to the stability of the system ([Yamasaki & Yajima, 2013, 2016]). The system is considered to be N-stable when $N > 0$, as N-unstable when $N < 0$, and as N-neutral when $N = 0$. Around the equilibrium points, J-stable and J-unstable correspond to a spiral and a node, respectively [Sabău, 2005a]. N-stable and N-unstable correspond to linear stable and linear unstable, respectively ([Yamasaki & Yajima, 2013, 2016]). For instance, J-stable and N-stable around the equilibrium point correspond to a stable spiral (see [Yamasaki & Yajima, 2013] for more details).

2.2. *Time-like potential and elementary catastrophe*

The subject of KCC theory is a second-order ODE; thus, KCC theory cannot be applied to a first-order ODE. Antonelli *et al.*, (1993) introduced the production process concept, which enables the application of KCC theory to first-order ODEs such as the logistic equation. This second-order logistic equation has been applied to the real growth data of several species ([Antonelli, 1985; Antonelli *et al.*, 1993]), and to

evolution in biology([Antonalli *et al.*, 2019, 2021]). The similar formulation has been also used to study transient behaviors during the production process, such as the effects of time feedback ([Hutchinson, 1948; Wright, 1955]). Moreover, Yamasaki and Yajima (2017) applied this technique to typical one-dimensional bifurcations described by first-order ODEs, such as saddle-node, transcritical, and pitchfork bifurcations, to obtain the same bifurcation as the original equation. Yamasaki and Yajima (2020) focused on the jump phenomenon (bifurcation), referred to as a catastrophic shift based on the time-like potential.

This paper defines x as a time-like potential of variable n. Time-like potentials do not always exist, because their existence essentially depends on properties of n such as integrability. In this paper, the variable n physically exists, whereas the time-like potential x is purely a mathematical construct. Therefore, it would be appropriate to express the analytical results in terms of n, rather than the time-like potential x. Specifically, this paper considers bifurcation stability, so it is appropriate to express the geometric quantities related to stability in terms of n. As we will see in the later section, the nonlinear connection related to N-stability and deviation curvature related to J-stability are expressed in terms of n in the last step. Thus, the time-like potential can be used as part of the analytical process, but is not necessary for the final interpretation of the bifurcation stability (see [Yamasaki & Yajima, 2020] for more details).

This paper applies the KCC theory to one-dimensional elementary catastrophe based on the time-like potential. We will show that the previous results can be obtained by an analysis based on the time-like potential. In addition, this approach allows for the analysis of non-equilibrium stability. Let us consider the dynamical system given by

$$\dot{n} = F(n), \tag{6}$$

where F is a function of n. This paper assumes that F and n satisfy the integrability conditions, so there is potential for f_c and x, as follows. In the elementary catastrophe, the potential function of the dynamical system, $f_c(n)$ is introduced as [Thom, 1972; Thompson, 1982]:

$$F = -\frac{\partial f_c}{\partial n} = -\partial_n f_c. \tag{7}$$

This paper uses the time-like potential defined by (e.g., [Antonelli *et al.*, 1993])

$$n = \frac{dx}{dt} = \dot{x}. \tag{8}$$

Therefore, this paper considers the equation:

$$\ddot{x} + \partial_n f_c(n) = 0. \tag{9}$$

That is, $g = \partial_n f_c(n)$ in the basic form of the KCC theory (1): $\ddot{x} + g = 0$. Therefore, the concrete forms of $f_c(n)$ give various differential geometrical quantities of the dynamical system. This paper considers the elementary catastrophe of one active variable given by the following, and the normal form [Thom, 1972; Poston, & Stewart, 1978]:

$$\text{Fold} : f_c(n) = \frac{n^3}{3} + an, \tag{10}$$

$$\text{Cusp} : f_c(n) = \frac{n^4}{4} + \frac{an^2}{2} + bn, \tag{11}$$

$$\text{Swallowtail} : f_c(n) = \frac{n^5}{5} + \frac{an^3}{3} + \frac{bn^2}{2} + cn, \tag{12}$$

$$\text{Butterfly} : f_c(n) = \frac{n^6}{6} + \frac{an^4}{4} + \frac{bn^3}{3} + \frac{cn^2}{2} + dn, \tag{13}$$

where a, b, c and d are parameters. Since the fold, i.e., saddle-node bifurcation, has already been considered [Yamasaki & Yajima, 2017], this paper will consider other types, specifically, the cusp, swallowtail, and butterfly. In the variable dynamical system with the time-like potential, the non-linear connection (4), Berwald connection (5), and deviation curvature (3) can be simplified as follows [Yamasaki & Yajima, 2017]:

$$N = \frac{1}{2}\partial_{\dot{x}} g = \frac{1}{2}\partial_n g, \tag{14}$$

$$G = \partial_{\dot{x}} N = \partial_n N, \tag{15}$$

$$P = -Gg + N^2. \tag{16}$$

For elementary catastrophe, the equation of the bifurcation curve is derived from the condition: $\partial_n f_c = 0$ and $\partial_n \partial_n f_c = 0$ [Thom, 1972]. From $g = \partial_n f_c$ and Eq. (14), this condition is expressed geometrically as

$$g = 0, N = 0. \tag{17}$$

In this section, the bifurcation curve is derived by this condition: N-stability is neutral ($N = 0$) in equilibrium state ($g = 0$). The other quantities G and P are not relevant in this case. However, we derive them here as they are necessary for the non-equilibrium analysis discussed in the following section.

First, we consider the cusp defined by Eq. (11). From $g = \partial_n f_c$, Eqs. (14), (15), and (16) give the following geometric quantities:

$$N = \frac{1}{2}(3n^2 + a), \tag{18}$$

$$G = 3n, \tag{19}$$

$$P = \frac{1}{4}(-3n^4 - 6an^2 - 12bn + a^2). \tag{20}$$

Therefore, Eq. (17) gives the parametric equations of the bifurcation curve: $\gamma(n) = (b, a) = (2n^3, -3n^2)$. The curve has a cusp, as shown in the upper part of Fig. 1. The details of the figure are described in Section 2.3. Let us check the type of singular point with calculations. $d\gamma/dn|_{n=0} = \gamma'(0) = 0$ shows that the point $n = 0$ is the singular point. At the singular point, we obtain $\det(r'', r''') \neq 0$. This means that the type of singular point is cuspidal [Porteous, 2001; Izumiya *et al.*, 2016].

Next, we consider the swallowtail defined by Eq. (12). The same calculation used for the cusp case gives

$$N = 2n^3 + an + \frac{1}{2}b, \tag{21}$$

$$G = 6n^2 + a, \tag{22}$$

$$P = -ac - 3an^4 + \frac{b^2}{4} - 4bn^3 - 6cn^2 - 2n^6. \tag{23}$$

Equation (17) gives $b = -4n^3 - 2an$ and $c = 3n^4 + an^2$. Therefore, the bifurcation curve is a swallowtail type, as shown in the upper part of Fig. 2. Because the curve is recognized as the cross-section of the wave front $f(n, a) = (3n^4 + an^2, -4n^3 - 2an, a)$, we can obtain the identifier of the singularity from $\partial_n f \times \partial_a f$, as follows [Saji & Teramoto, 2020]: $\Lambda = 6n^2 + a$. At the singular point $n = 0$, we have $\partial_n \Lambda = 0$ and $\partial_n \partial_n \Lambda \neq 0$. This means that the type of singular point is swallowtail [Kokubo *et al.*, 2005; Fujimori *et al.*, 2008; Saji *et al.*, 2009; Izumiya *et al.*, 2010].

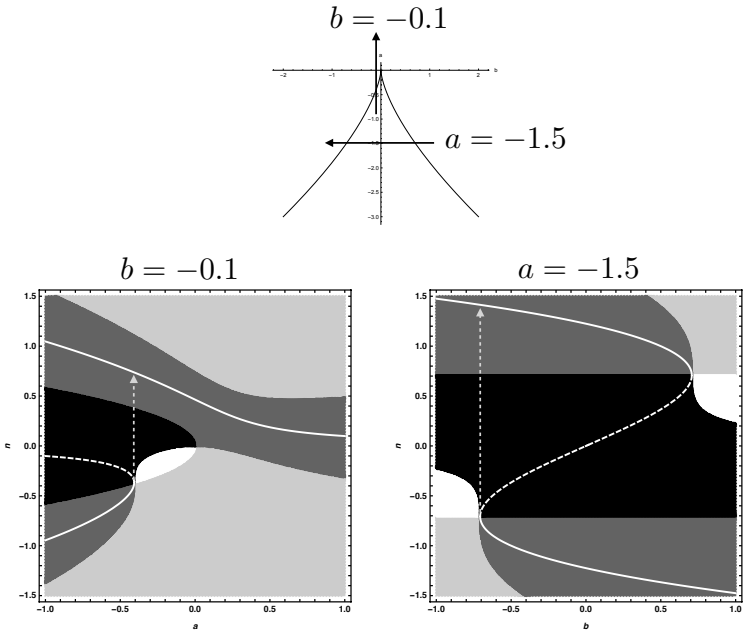

Fig. 1. Upper part shows the bifurcation curve with the cusp obtained by the condition $g = 0, N = 0$, i.e., the N-stability is neutral in the equilibrium state. By fixing the parameter, we obtain the lower part of the figure that shows the stable equilibrium curve (white solid line), the unstable equilibrium curve (white dotted line), and the KCC stability region described by the following gray-scale. The white region shows N-unstable and J-stable parts; the black region shows N-unstable and J-unstable parts; the light-gray region shows N-stable and J-stable parts; and the dark-gray region shows N-stable and J-unstable parts.

Finally, we consider the butterfly defined by Eq. (13). The same calculation used for the cusp case gives

$$N = \frac{1}{2}\left(3an^2 + 2bn + c + 5n^4\right), \tag{24}$$

$$G = 10n^3 + 3an + b, \tag{25}$$

$$P = \frac{1}{4}\left(3an^2 + 2bn + c + 5n^4\right)^2 - \left(3an + b + 10n^3\right)\left(an^3 + bn^2 + cn + d + n^5\right). \tag{26}$$

Equation (17) gives $c = -3an^2 - 2bn - 5n^4$ and $d = n^2\left(2an + b + 4n^3\right)$. Therefore, the bifurcation curve is of the butterfly type, as shown in the upper part of Fig. 3. The identifier of the singularity is given by $\Lambda = 10n^3 + b$ when $a \to 0, c \to -c$. This satisfies $\partial_n\Lambda(p) = \partial_n\partial_n\Lambda(p) = 0$ and $\partial_n\partial_n\partial_n\Lambda(p) \neq 0$ at the singular point p, so the singular point is a butterfly type [Izumiya, & Saji, 2010; Izumiya *et al.*, 2010].

As mentioned above, geometrical quantities related to stability, such as N, G, and P, are expressed in terms of n in the last step, so this paper uses the time-like potential as part of the analytical process. However, this does not mean that the time-like potential is always a purely mathematical concept, even in other analyses. Especially with unusual phenomena in which production processes (history) predominate, it becomes an explicit quantity. For instance, if we consider the number of paleontological species as n, the number of fossils x observed in the stratum that formed during sedimentation is proportional to the time integral of n (e.g., [Raup & Stanley, 1978]). The differential form of this relationship corresponds to Eq. (8). Another example is the free rotation of a rigid body system, in which n corresponds to angular velocities and x corresponds to the Euler angles; here, the general form of Eq. (8) reveals the non-holonomic geometric structures of a rigid body system [Yajima *et al.*, 2018].

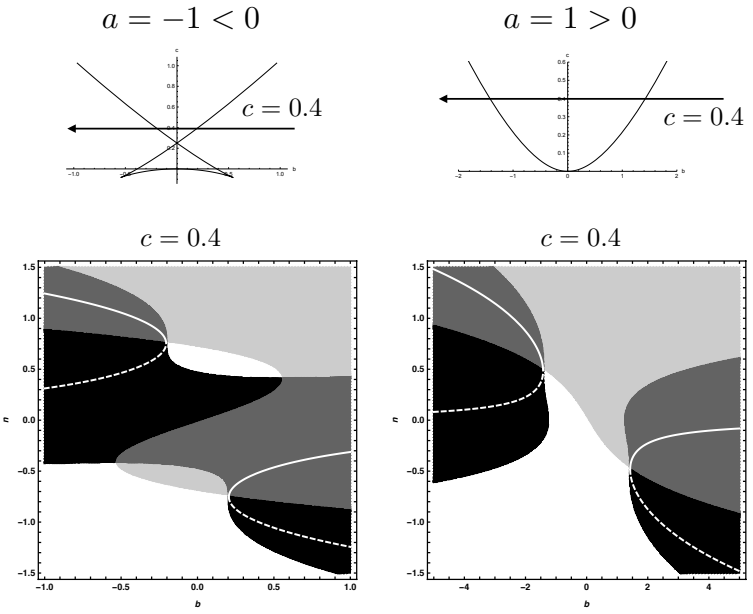

Fig. 2. Upper part shows the bifurcation curve with the swallowtail. The lower part is obtained by fixing the parameter and shows the KCC stability.

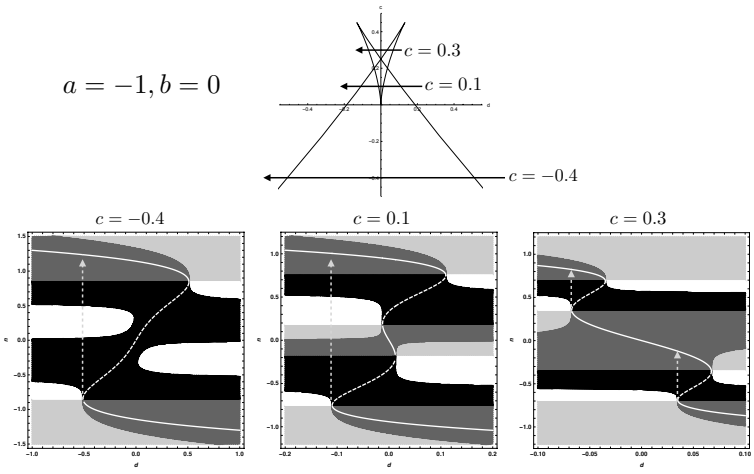

Fig. 3. Upper part shows the bifurcation curve with the butterfly. The lower part is obtained by fixing the parameter and shows the KCC stability.

2.3. *KCC stability of elementary catastrophe*

The upper parts of Figs. 1-3 show bifurcation curves with singularities in elementary catastrophe. The lower parts show the equilibrium curves (white solid and dotted lines) and the geometric stability in the non-equilibrium region (gray-scale region). The white solid line shows the stable equilibrium, and the white dotted line shows the unstable equilibrium. The white region shows N-unstable and J-stable parts; the black region shows N-unstable and J-unstable parts; the light gray region shows N-stable and J-stable parts; and the dark gray region shows N-stable and J-unstable parts. In the following paragraphs, we will look at the details of each figure. As the equilibrium results are similar, the difference in singularity can be seen by focusing on non-equilibrium stability, i.e., KCC analysis.

Figure 1 shows the bifurcation curve given by the set of coefficients (a, b) satisfying Eq. (17), which is confirmed to be cusp. The figure below shows the KCC stability of the cusp based on Eqs. (18) and (20).

Fixing $b = -0.1$ and crossing the cusp from bottom to top is the left side of the lower part of Fig. 1. This is a typical example of an incomplete bifurcation, i.e., the equilibrium curve (white curve) has separated into two parts. This separated region is the non-equilibrium region because it extends between the equilibrium curves. Equations (18) and (20) allow us to express the stability of this separated region (non-equilibrium region) as the gray scale. As the parameter a increases, a catastrophe occurs on the left side of the cusp (dotted arrow). Fixing $a = -1.5$ and crossing the cusp from right to left is the right side of the lower part of Fig. 1. Similarly, a catastrophe occurs on the left side of the cusp (dotted arrow). In both cases, the dotted arrow goes from the black region through the dark gray region. This is a typical result of stability change during the catastrophe process, as described in earlier works [Yamasaki & Yajima, 2020].

Figure 2 shows the bifurcation curve given by the set of coefficients (b, c) satisfying Eq. (17), which is confirmed to be swallowtail ($a < 0$) and fold ($a > 0$). The figure below shows the KCC stability based on Eqs. (21) and (23). Fixing $c = 0.4$ and crossing the bifurcation curves, the equilibrium curve (white curve) shows a similar separation pattern for $a < 0$ (Fig. 2 left) and $a > 0$ (Fig. 2 right), but the stability of the non-equilibrium region (gray scale) is different.

Figure 3 shows the bifurcation curve given by the set of coefficients (d, c) satisfying Eq. (17), which is confirmed to be butterfly. The figure below shows the KCC stability based on Eqs. (24) and (26). Since b is bias parameter [Bröcker, & Lander, 1975], we set $b = 0$ for simplicity in Fig. 3. Moreover, since case $a > 0$ is essentially the same as a cusp, we will only analyze case $a < 0$. The bending pattern of the equilibrium curve in the lower left of Fig. 3 ($c = -0.4$) is typical in catastrophe phenomena. For instance, the cusp in the lower right of Fig. 1 ($a = -1.5$) shows a similar bending pattern. However, the stability of the non-equilibrium region, i.e., during the catastrophe process (dotted arrow), can vary as follows. The arrow on the lower left of Fig. 3 ($c = -0.4$) passes through the white region. At the bottom center of Fig. 3 ($c = 0.1$), the arrow passes through the light gray region (N-stable and J-stable). It is interesting that the most stable region exists in the non-equilibrium region. The bottom right of Fig. 3 ($c = 0.3$) shows a pattern unique to butterfly, where two catastrophic shifts occur. This is different from the others, but the non-equilibrium region is a typical pattern, i.e., transition from a black to dark-gray region.

2.4. *Douglas tensor of elementary catastrophe*

The analysis in the previous section shows that non-equilibrium stability during the catastrophic shift can vary, even though the pattern of the equilibrium curve is similar. Previous analyses have shown that the Douglas tensor is useful for describing stability changes during catastrophic shifts [Yamasaki & Yajima, 2020]; thus, here we apply the method to elementary catastrophe. We can see that just as KCC stability is represented by the combination of the non-linear connection N and deviation curvature P, changes in KCC stability during the shift are represented by the combination of the Berwald connection G and Douglas tensor D.

The catastrophic shifts shown in Figs. 1-3 occur in the vertical (n-axis direction); thus, it is necessary to consider the change in stability along the n-axis. Then, we consider the expression of P (J-stability) differentiated into n [Yamasaki & Yajima, 2020]:

$$\frac{dP}{dn} = D\frac{dn}{dt}, \tag{27}$$

where D is the Douglas tensor [Douglas, 1927]. The Douglas tensor is one of the invariants of KCC theory (Douglas, 1927). In one-dimensional space, it is defined by $D = \partial_n G$; thus, combining Eqs. (1), (3), (4), and (5) gives Eq. (27). Because this contains dn/dt, it is essentially an equation for the non-equilibrium region. Geometrically, this equation shows that the Douglas tensor affects the deviation curvature during a catastrophic shift. In the one-dimensional case, $D = \partial_n G$, so calculating D for each catastrophe from (19), (22), and (25) gives

$$D_{\text{cusp}} = 3, \tag{28}$$

$$D_{\text{swallowtail}} = 12n, \tag{29}$$

$$D_{\text{butterfly}} = 30n^2 + 3a. \tag{30}$$

$D_{\text{butterfly}}$ contains the parameter a. When $a > 0$ i.e., $D > 0$, it is the same as the cusp. When $a < 0$, it can be factored as $D = 30(n + \sqrt{-a/10})(n - \sqrt{-a/10})$, such that $dP/dn < 0$ is valid. Therefore, even if $P > 0$ at the start of the shift (i.e., equilibrium point), there can be regions where $P < 0$ during the shift (i.e., non-equilibrium region/s). For instance, we see the shift of the lower left of Fig. 3, in which $c = -0.4$, $d \approx -0.51$, and $dn/dt > 0$ (arrow direction). The calculations show that the range $dP/dn < 0$ is $-0.32 < n < 0.32$ from $D \propto (n + 0.32)(n - 0.32)$, and the range $P < 0$ is $0.026 < n < 0.51$ from Eq. (26).

In a similar fashion, the Berwald connection $G = \partial N/\partial n$ controls N-stability during catastrophic shifts. In the case of butterfly without "bias" (i.e., $b = 0$), the Berwald connection is given by $G = 3an + 10n^3$. As shown in the center of Fig. 3, when $c = 0.1$ and there is a shift, $dn/dt > 0$; thus, from the calculations, the range $\partial N/\partial n > 0$ is $-0.55 < n < 0$ and $n > 0.55$ from $G \approx 10(n+0.55)n(n-0.55)$, and the range $N > 0$ is $-0.19 < n < 0.19$ and $n > 0.75$ from (24). An N-stable region exists in non-equilibrium, $-0.19 < n < 0.19$; thus, the light-gray region (N-stable and J-stable) can exist in the range $0.01 < n < 0.19$.

As can be seen from Eqs. (28) and (29), the Douglas tensor for cusp and swallowtail are either constant or linear in n, such that the stability pattern during a catastrophic shift is not as complicated as for the butterfly above.

3. Non-equilibrium singular point of the Hill function

3.1. *Bifurcation curve and differential geometrical quantities*

In ecology, the logistic equation with the Hill function is a typical example of a catastrophe [Ludwig *et al.*, 1978; Scheffer et al., 2009; Strogatz, 2014]. KCC analysis, however, shows that its bifurcation curve has different characteristics from the elementary catastrophe considered in Section 2, as shown below. As mentioned in Section 2.2, this paper considers the following dynamical system:

$$\dot{n} + g = 0, \tag{31}$$

where $g = \partial_n f_c(n)$ with f_c as the potential function. The potential function of the logistic equation is $(n^3 r)/(3K) - (n^2 r)/2$, and that of the Hill function is $n - \tan^{-1}(n)$ from $n^2/(1 + n^2) = 1 - 1/(1 + n^2)$. Therefore, the potential function f_c of the logistic equation with the Hill function is given by

$$f_c = \frac{n^3 r}{3K} - \frac{n^2 r}{2} + n - \tan^{-1}(n).$$

In ecology, n, r, and K are all positive and correspond to biomass, the growth rate, and the carrying capacity, respectively. The potential f_c has the following known form:

$$g = \partial_n f_c = -rn + \frac{r}{K} n^2 + \frac{n^2}{1 + n^2}. \tag{32}$$

Therefore, Eqs. (14), (15), and (16) give the differential geometrical quantities of the system:

$$N = n\left(\frac{r}{K} + \frac{1}{(n^2+1)^2}\right) - \frac{r}{2}, \tag{33}$$

$$G = \frac{r}{K} + \frac{1 - 3n^2}{(n^2+1)^3}, \tag{34}$$

$$P = -\frac{n^3 r\left(4K + n^3 - 3n\right)}{K\left(n^2+1\right)^3} + \frac{3n^4}{(n^2+1)^4} + \frac{r^2}{4}. \tag{35}$$

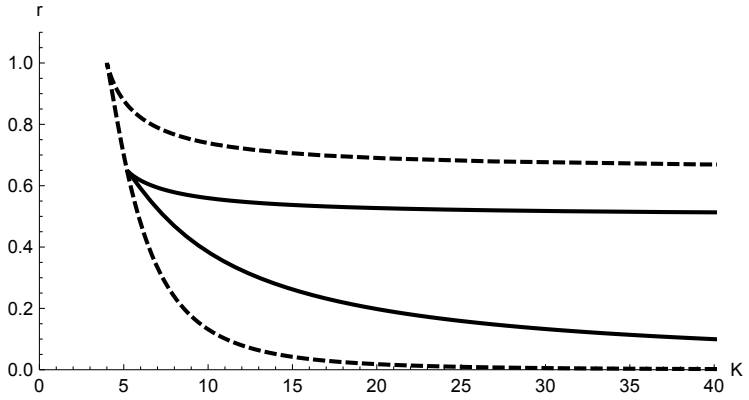

Fig. 4. Two bifurcation curves with cusps obtained by the condition: $N = 0, P = 0$, i.e., the stability is neutral. The solid line is the equilibrium curve ($G|_{N_0P_0} \neq 0$) given by Eq. (36). The dotted line is the non-equilibrium curve ($G|_{N_0P_0} = 0$) given by Eq. (37).

Yamasaki and Yajima (2020) showed that when $N = 0$ and $P = 0$, i.e., the geometrical stability is neutral, we can obtain the parametric equations of the bifurcation curve. Let K, r that satisfies the conditions of $N = 0$ and $P = 0$ be K_0, r_0. In this case, Eqs. (33) and (35) give the following two bifurcation curves:

$$\gamma(K_0, r_0) = \left(\frac{2n^3}{n^2 - 1}, \frac{2n^3}{(n^2 + 1)^2} \right), \tag{36}$$

or

$$\gamma(K_0, r_0) = \left(\frac{8n^3}{3n^2 - 1}, \frac{8n^3}{(n^2 + 1)^3} \right). \tag{37}$$

Figure 4 shows the parametric plots of Eqs. (36) and (37). The cusp is observed in both cases. The solid line given by Eq. (36) agrees with the known bifurcation curve (e.g., [Strogatz, 2014]). The dotted line given by Eq. (37) is the new bifurcation curve obtained from KCC analysis. Yamasaki and Yajima (2020) did not provide a sufficient reason for the existence of this new solution (37); thus, we consider it here. Based on this consideration, the concept of bifurcation curves in non-equilibrium states will be presented. This bifurcation curve has a singular point, which implies the existence of a singular point in the non-equilibrium state.

3.2. *Non-equilibrium singular point*

As described in Section 2.2, the bifurcation curve of the dynamical system can be derived by (17): $g = 0, N = 0$. From $\dot{n} + g = 0$, this gives $\dot{n} = 0$, i.e., an equilibrium state. Moreover, Eq. (16): $P = -Gg + N^2$ shows $P = 0$. Therefore, the bifurcation curve in equilibrium satisfies the following equation:

$$N = 0, P = 0. \tag{38}$$

Conversely, let us consider the bifurcation curve starting from condition (38). From $P = -Gg + N^2$, this means $Gg = 0$. Let the parametric set that satisfies the condition (38) be N_0P_0. For instance, the components (K_0, r_0) in Eqs. (36) and (37) correspond to this. The equation $Gg = 0$ means three combinations:

$$g|_{N_0P_0} = 0, \ G|_{N_0P_0} \neq 0, \tag{39}$$

$$g|_{N_0P_0} \neq 0, \ G|_{N_0P_0} = 0, \tag{40}$$

$$g|_{N_0P_0}= G|_{N_0P_0}= 0. \tag{41}$$

The relation (39) gives a known equilibrium bifurcation curve, as described earlier. In this case, the Berwald connection G is generally non-zero. When G vanishes, the relation (40) holds and gives another bifurcation curve. Since $g \neq 0$ means $\dot{n} \neq 0$, this is in the non-equilibrium state. The relation (41) does not hold in general, but is valid at the equilibrium singular point. Equations (40) and (42) describe the geometric relation for the usual singularity in the equilibrium state, while Eq. (41) pertains to the non-equilibrium states. We cannot discuss non-equilibrium singularities without considering the Berwald connection introduced by KCC theory.

Let us check the above results using the Hill function. The substitution of the parametric set satisfies (38), i.e., the components of (36) into (32) and (34) gives the relation (39):

$$g|_{K_0,r_0}= 0, \quad G|_{K_0,r_0}= \frac{n^2\left(n^2-3\right)}{\left(n^2+1\right)^3}. \tag{42}$$

Since $\dot{n} = 0$ from $\dot{n} + g = 0$, it is confirmed that the known solution (36) is the bifurcation curve in equilibrium. The substitution of the components of (37) into (32) and (34) gives the relation (40):

$$g|_{K_0,r_0}= \frac{n^4\left(n^2-3\right)}{\left(n^2+1\right)^3}, \quad G|_{K_0,r_0}= 0. \tag{43}$$

Since $\dot{n} \neq 0$ in general, the new solution (37) is the bifurcation curve in non-equilibrium. Thus, the condition $N = 0, P = 0$ in the KCC theory encompasses not only the known equilibrium bifurcation curve (36), but also the non-equilibrium bifurcation curve (37). As can be seen from Fig. 4, the bifurcation curve (36) and (37) are tangent at the equilibrium singular point $n = \sqrt{3}$. At the point, $G|_{K_0,r_0}$ in (42) and $g|_{K_0,r_0}$ in (43) become zero, such that the relation (41) holds.

Let us consider the condition under which two bifurcation curves can be obtained, such as (36) and (37). Two equations for the bifurcation curve require a quadratic equation for the coefficients. Since the nonlinear connection is linear with respect to g from $N = (1/2)\partial_n g$, the equation $N = 0$ does not correspond to this. On the other hand, from $P = -Gg + N^2$, the deviation curvature contains a nonlinear term, so the equation $P = 0$ is needed for two bifurcation curves. Moreover, the coefficients of the variables are important because they remain after differentiation by n. In other words, when considering the coefficients of the constant term, only one bifurcation curve is obtained (examples will be given in Section 4). In the case of the Hill function, the relation (40) can be obtained because Eq. (32) shows that all of the coefficients K, r are on the variable n. Usually, if there is a single bifurcation curve, it is an equilibrium one.

3.3. *Cuspidal curvature of a non-equilibrium singular point*

In Fig. 4, both equilibrium and non-equilibrium singular points appear to be cusps. This can be confirmed using the discriminant condition [Porteous, 2001]. The results of this calculation can be used to estimate curvature at the singular point [Umehara, 2011; Saji *et al.*, 2010; Shiba & Umehara, 2012]. This is useful for quantifying the differences between equilibrium and non-equilibrium cusps.

First, we consider the equilibrium bifurcation curve (36). The derivative gives

$$\frac{d\gamma}{dn} = \gamma' = \left\{ \frac{2n^2\left(n^2-3\right)}{\left(n^2-1\right)^2}, -\frac{2n^2\left(n^2-3\right)}{\left(n^2+1\right)^3} \right\}. \tag{44}$$

This is zero at $n = \sqrt{3}$ in $n > 0$, so it is the singular point. Moreover, $\det(\gamma'', \gamma''')$ gives

$$\begin{vmatrix} \frac{4n\left(n^2+3\right)}{\left(n^2-1\right)^3} & \frac{4n\left(n^4-8n^2+3\right)}{\left(n^2+1\right)^4} \\ -\frac{12\left(n^4+6n^2+1\right)}{\left(n^2-1\right)^4} & -\frac{12\left(n^6-15n^4+15n^2-1\right)}{\left(n^2+1\right)^5} \end{vmatrix} = \frac{192n^3\left(3n^6-7n^4-27n^2+15\right)}{\left(n^2-1\right)^4\left(n^2+1\right)^5}. \tag{45}$$

This is not zero at $n = \sqrt{3}$. Since $\gamma' = 0$ and $\det(\gamma'', \gamma''') \neq 0$ at the singular point, the discriminant condition shows that the type of equilibrium singular point is cusp [Porteous, 2001; Izumiya *et al.*, 2016].

In a similar fashion, the non-equilibrium bifurcation curve (37) gives γ' and $\det(\gamma'', \gamma''')$ as follows:

$$\left\{ \frac{24n^2\left(n^2-1\right)}{\left(1-3n^2\right)^2}, -\frac{24n^2\left(n^2-1\right)}{\left(n^2+1\right)^4} \right\}, \tag{46}$$

$$\begin{vmatrix} \frac{48\left(n^3+n\right)}{\left(3n^2-1\right)^3} & \frac{48\left(2n^5-5n^3+n\right)}{\left(n^2+1\right)^5} \\ -\frac{48\left(9n^4+18n^2+1\right)}{\left(1-3n^2\right)^4} & -\frac{48\left(10n^6-45n^4+24n^2-1\right)}{\left(n^2+1\right)^6} \end{vmatrix} = -\frac{9216n^3\left(3n^6-34n^4+49n^2-10\right)}{\left(1-3n^2\right)^4\left(n^2+1\right)^5}. \tag{47}$$

At the singular point $n = 1$ ($\gamma' = 0$), we have $\det(\gamma'', \gamma''') \neq 0$. Therefore, the non-equilibrium singular point is also a cusp.

From the above calculations, it is confirmed using the Hill function that both the equilibrium and non-equilibrium singular points are cusp type. Of course, this has only been confirmed with the Hill function; in general, it is possible to have different types of singular points (e.g., swallowtail or butterfly). In fact, examples of this are provided in the next section.

Catastrophe theory, which was introduced in the 1960s, has influenced various research areas (e.g., singularity theory). Recently, Umehara (2011) introduced the new concept of singular curvature at the cusp. Saji et al. (2010) considered cuspidal curvature based on the duality between singular points and inflection points. According to recent studies, we can characterize the system in terms of curvature even at the singular point [Umehara, 2011; Saji *et al.*, 2010; Shiba & Umehara, 2012]. Thus, we estimate the curvature of the two singular points in Fig. 4 and show that they are the same in terms of quality (both cusp) but differ in quantity. When the curve $\gamma(n)$ has a cusp at $n = c$, the cuspidal curvature is defined as [Saji *et al.*, 2010; Shiba & Umehara, 2012] :

$$\mu = \frac{\det(\gamma''(c), \gamma'''(c))}{|\gamma''(c)|^{5/2}}. \tag{48}$$

Since $\det(\gamma'', \gamma'') \neq 0$ at the cusp, the cuspidal curvature is always non-zero. If the sign of the curvature is positive (negative), it is called zig (zag), and the bifurcation curve turns to the right (left) of the growth direction at the singular point (Fig. 4.1 in [Saji *et al.*, 2010]). The sign is invariant under an orientation preserving diffeomorphism of the plane [Shiba & Umehara, 2012]. That is, the sign changes when the orientation of the curve is reversed. The magnitude of the curvature indicates the degree of opening of the cusp. The number $(1/\mu)^2$ is called the cuspidal curvature radius, which corresponds to the radius of the best approximating cycloid at the cusps ([Saji *et al.*, 2010; Shiba & Umehara, 2012]).

Using the results of Eqs. (45) and (47), Eq. (48) indicates that the cuspidal curvature of the equilibrium singular point is about -0.047 and that of the non-equilibrium singular point is about -0.27. The difference in magnitude of cuspidal curvature reflects the difference in the degree of the opening of the two bifurcation curves, as shown in Fig. 4. This enclosed area is the so-called bistable state, where rapid changes in biomass occur [Ludwig *et al.*, 1978; Scheffer et al., 2009; Strogatz, 2014]. Thus, this phenomenon occurs over a wider range of parameters in the non-equilibrium regime. In this way, calculation of the cuspidal curvature at the singular point is useful for identifying the range of bistable states in parametric space.

As mentioned above, studies of singular curvature are mainly mathematical. Therefore, it is useful to show that singular curvature is also applicable to natural science and gives an important perspective. For instance, the range of bistable states of the ecosystem, and usually changes with the form of the equation. However, the results of this paper show that the cusp curvature of the non-equilibrium state is larger than that of the equilibrium state. Thus, the range of bistable states is increased simply by shifting the system from an equilibrium state to a non-equilibrium state, even if the equation itself does not change. It has long been accepted that actual ecosystems may be in a state of non-equilibrium [Pickett, 1980; Sprugel, 1991; Mori, 2011]; thus, singularity curvature is useful for interpreting the diversity of ecosystems.

In the above, only cuspidal curvature is considered; however, there are various geometric invariants that characterize a singular point, such as cusp-directional torsion, singular curvature, and so on[Saji *et al.*, 2009; Hasegawa *et al.*, 2015; Martins, & Saji, 2016; Martins *et al.*, 2016]. Based on these geometric quantities, a more detailed analysis of the singular point of the ecosystem is a future research target.

4. Non-equilibrium singular point of elementary catastrophe

In Section 2, we analyzed the singular points of elementary catastrophe from the geometrical expression of known viewpoints as (17): $g = 0, N = 0$, i.e., the N-stability is neutral in equilibrium. In this section, we reanalyze it from the viewpoint obtained in Section 3 as (38): $N = 0, P = 0$, i.e., stability is neutral. The latter viewpoint does not include g; thus, it does not matter whether it is in equilibrium or not. Since the bifurcation curve is related to linear stability, the neutral condition for N-stability ($N = 0$) is necessary for both viewpoints. Moreover, one more equation is needed to obtain two variables describing the bifurcation curve. The previous analysis used the equilibrium state ($g = 0$), whereas here we use the J-stability ($P = 0$). Since the deviation curvature P is introduced by KCC theory, the theory is useful for considering the non-equilibrium singular point.

4.1. *Cusp*

We will show that the normal form of a cusp contains only an equilibrium singular point. The dynamical system with a cusp is $\dot{n} + g = 0$ with

$$g = n^3 + an + b. \tag{49}$$

Thus, as obtained in Section 2.2, the differential geometric quantities of cusp can be obtained from equations (14), (15), and (16). For convenience, we redescribe the results:

$$N = \frac{1}{2}(3n^2 + a), \quad G = 3n, \quad P = \frac{1}{4}(-3n^4 - 6an^2 - 12bn + a^2). \tag{50}$$

Therefore, the solutions (a_0, b_0) of (38): $N = 0, P = 0$, give the following bifurcation curve:

$$\gamma(a_0, b_0) = (-3n^2, 2n^3). \tag{51}$$

This is the known equilibrium bifurcation curve of cusp (Fig. 1). In fact, from (51), $g|_{a_0,b_0} = 0$ and $G = 3n$ is generally non-zero, so the relation (39) is satisfied.

4.2. *Swallowtail*

The dynamical system with swallowtail is $\dot{n} + g = 0$ with

$$g = n^4 + an^2 + bn + c. \tag{52}$$

We redescribe the differential geometric quantities of swallowtail obtained in Section 2.2:

$$N = 2n^3 + an + \frac{1}{2}b, \quad G = 6n^2 + a, \quad P = -ac - 3an^4 + \frac{b^2}{4} - 4bn^3 - 6cn^2 - 2n^6. \tag{53}$$

Therefore, from the solutions (b_0, c_0) of (38),

$$\gamma(b_0, c_0) = (-2(an + 2n^3), n^2(a + 3n^2)). \tag{54}$$

This gives the known equilibrium bifurcation curve of swallowtail (Fig. 2). From $g|_{b_0,c_0} = 0, G|_{b_0,c_0} = 6n^2 + a$, the relation (39) is satisfied. In the (b, c)-space of swallowtail, the identifier of singularity Λ is equal to

the Berwald connection G, so the vanishing condition $\Lambda = 0$ at the equilibrium singular point corresponds to the relation (41). In this case, the condition of discrimination (differentiation of Λ) is related to the Douglas tensor.

Next, we consider the solutions (a_0, c_0) of (38):

$$\gamma(a_0, c_0) = \left(\frac{-b - 4n^3}{2n}, \frac{1}{2}\left(2n^4 - bn\right) \right). \tag{55}$$

Since $g|_{a_0,c_0} = 0, G|_{a_0,c_0} = 4n^2 - b/2n$, this also gives the equilibrium bifurcation curve.

Finally, we consider that the combination does not contain a coefficient of the constant term: c, that is, (a, b). In this case, we can obtain two solutions of Eq. (38):

$$\gamma(a_0, b_0) = \left(-6n^2, 8n^3\right), \tag{56}$$

$$\gamma(a_0, b_0) = \left(\frac{c - 3n^4}{n^2}, \frac{2\left(n^4 - c\right)}{n} \right). \tag{57}$$

The curve (56) gives $g|_{a_0,b_0} = c + 3n^4$, $G|_{a_0,b_0} = 0$, i.e., the relation (40), so it is a non-equilibrium one. Therefore, the point $n = 0$ is a non-equilibrium cusp. The curve (57) gives $g|_{a_0,b_0} = 0, G|_{a_0,b_0} = (c+3n^4)/n^2$, i.e., the relation (39); thus, it is an equilibrium one.

4.3. *Butterfly*

The dynamical system with butterfly is $\dot{n} + g = 0$ with

$$g = n^5 + an^3 + bn^2 + cn + d. \tag{58}$$

We redescribe the differential geometric quantities of butterfly obtained in Section 2.2:

$$N = \frac{1}{2}\left(3an^2 + 2bn + c + 5n^4\right), \tag{59}$$

$$G = 10n^3 + 3an + b, \tag{60}$$

$$P = \frac{1}{4}\left(3an^2 + 2bn + c + 5n^4\right)^2 - \left(3an + b + 10n^3\right)\left(an^3 + bn^2 + cn + d + n^5\right). \tag{61}$$

Therefore, the solutions (c_0, d_0) of (38) give

$$\gamma(c_0, d_0) = \left(-3an^2 - 2bn - 5n^4, n^2\left(2an + b + 4n^3\right)\right). \tag{62}$$

This gives the known equilibrium bifurcation curve for a butterfly type (Fig. 3). In fact, this gives $g|_{c_0,d_0} = 0, G|_{c_0,d_0} = 10n^3 + 3an + b$. As in the swallowtail case, the identifier of singularity in (c, d)-space is equal to the Berwald connection.

In the following, we consider combinations that do not contain a coefficient of the constant term: d. The solutions (a_0, b_0) of (38) give the equilibrium curve $(g|_{a_0,b_0} = 0, G|_{a_0,b_0} = (3d + cn + 3n^5)/n^2)$:

$$\gamma(a_0, b_0) = \left(\frac{cn + 2d - 3n^5}{n^3}, \frac{-2cn - 3d + 2n^5}{n^2} \right), \tag{63}$$

and the non-equilibrium curve $(g|_{a_0,b_0} = (3d + cn + 3n^5)/3, G|_{a_0,b_0} = 0)$:

$$\gamma(a_0, b_0) = \left(\frac{c - 15n^4}{3n^2}, \frac{5n^4 - c}{n} \right). \tag{64}$$

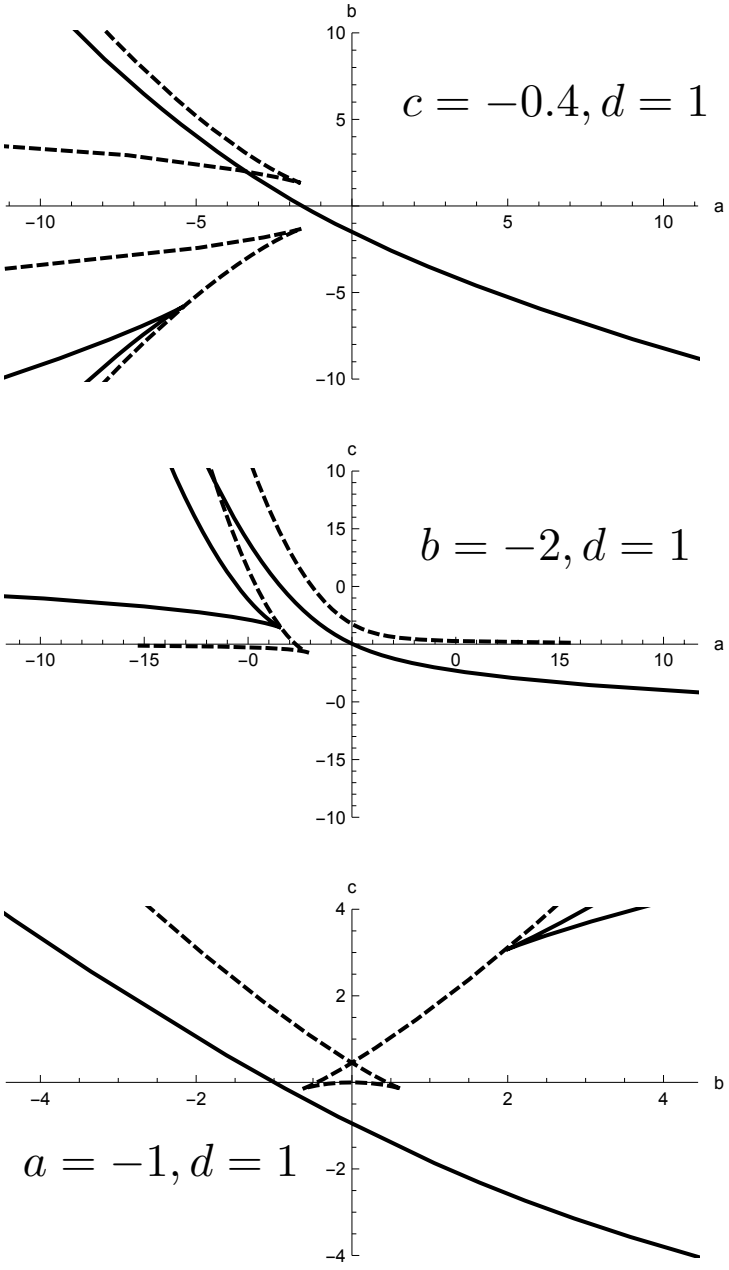

Fig. 5. Bifurcation curves for the combination of parameters do not contain a coefficient for the constant term d. The upper part is the parametric space (a_0, b_0), the middle part is (a_0, c_0), and the lower part is (b_0, c_0). In each space, the solid line is the equilibrium bifurcation curve, and the dotted line is the non-equilibrium one.

For instance, if we consider the case of $c = -0.4, d = 1$ (upper of Fig. 5), the equilibrium curve (solid line) gives one cusp, whereas the non-equilibrium curve (dotted line) gives two cusps. The solutions (a_0, c_0) of (38) give the equilibrium curve ($g|_{a_0,c_0} = 0, G|_{a_0,c_0} = -b/2 + 3d/2n^2 + 4n^3$):

$$\gamma(a_0, c_0) = \left(\frac{-bn^2 + d - 4n^5}{2n^3}, \frac{-bn^2 - 3d + 2n^5}{2n} \right), \tag{65}$$

and the non-equilibrium curve ($g|_{a_0,c_0} = (2/3)n^2(-b/2 + 3d/2n^2 + 4n^3), G|_{a_0,c_0} = 0$):

$$\gamma(a_0, c_0) = \left(\frac{-b - 10n^3}{3n}, 5n^4 - bn \right). \tag{66}$$

For instance, if we consider the case of $b = -2, d = 1$ (middle of Fig. 5), both curves (solid line and dotted line) have one cusp. The solutions (b_0, c_0) of (38) give the equilibrium curve $(g|_{b_0,c_0}= 0, G|_{b_0,c_0}= d/n^2 + an + 6n^3)$:

$$\gamma(b_0, c_0) = \left(\frac{-2an^3 + d - 4n^5}{n^2}, \frac{an^3 - 2d + 3n^5}{n} \right), \tag{67}$$

and the non-equilibrium curve $(g|_{b_0,c_0}= n^2(d/n^2 + an + 6n^3), G|_{b_0,c_0}= 0)$:

$$\gamma(b_0, c_0) = (-3an - 10n^3, 3(an^2 + 5n^4)). \tag{68}$$

For instance, if we consider the case of $a = -1, d = 1$ (lower part of Fig. 5), the equilibrium curve (solid line) gives one cusp and the non-equilibrium curve (dotted line) gives swallowtail.

The above results show that although the equilibrium bifurcation curve has one cusp regardless of the parameters, the non-equilibrium bifurcation curve shows singular points that vary depending on the parameters. This implies that the non-equilibrium singular points clarify the properties of catastrophe in each parametric space. Moreover, bifurcation curves with non-equilibrium singular points are expected to produce a diverse range of dynamical phenomena in nature. Usually, qualitative changes in the singularity are accompanied by changes in the parameters. The lower part of Fig. 5 shows that there are cases where the type of singularity changes from cusp to swallowtail, simply by changing from equilibrium to non-equilibrium, even if the parameters do not change. Although singularity analysis is often performed near the equilibrium point, this result indicates that non-equilibrium analysis, i.e. KCC theory, provides a useful perspective for analyzing singularity theory.

5. Conclusions

Our main conclusions are as follows.

(1) KCC theory is applied to three kinds of singularities in elementary catastrophe theory; these singularities show various stabilities in the non-equilibrium region (Sections 2.2 and 2.3; Figs. 1 – 3). Although the equilibrium curves of the cusp and butterfly show the same bending type, the change in stability during the shift (i.e., the non-equilibrium state) is different (Section 2.4. Table 1). Therefore, the differences in singularities become clearer when the analysis focuses on non-equilibrium stability, i.e., KCC analysis. Additionally, not only the stabilities, but also their changes during the shift, can be described by the basic geometric quantities in KCC theory (Table 2).

(2) We have shown that the typical bifurcation curve can be derived from the neutrality of N-stability in equilibrium (Section 2.2). We have also derived new types of bifurcation curves by considering the neutrality of both J-stability and N-stability (Sections 3.1 and 3.2). Because P contains a nonlinear term, its neutral condition is quadratic, so two bifurcation curves can be derived. In this case, a non-equilibrium bifurcation curve is derived from the vanishing condition of the Berwald connection (Table 3). This curve contains a singularity, suggesting the existence of a non-equilibrium singularity. Given that J-stability is unique to KCC theory, this result implies that KCC theory is useful for extending the singularity theory to non-equilibrium fields. Just as singularities are closely related to ordinary bifurcations, non-equilibrium singularities are closely related to non-equilibrium bifurcations.

(3) In the case of Hill functions, the cuspidal curvature of a non-equilibrium singular point is larger than that of an equilibrium singular point (Section 3.3). Biologically, this is interpreted as follows: the range of bistability of the ecosystem in the non-equilibrium state is greater than that in the equilibrium state. This means that the range of bistable states increases as the system shifts from equilibrium to non-equilibrium, even if the equation itself does not change (Fig. 4). Since the ecosystem is sometimes in non-equilibrium, calculation of the curvature of each singularity (equilibrium and non-equilibrium) is useful for understanding the diversity in nature.

(4) The singular points in equilibrium and non-equilibrium bifurcation curves are not necessarily the same (Section 4, Fig. 5). For instance, in the case of a butterfly type, the former is always a cusp, whereas the

latter varies depending on the parametric space. This means that even if the parameters do not change, there are cases where the type of singularity changes when the system shifts from an equilibrium to non-equilibrium state (Table 4). Therefore, the existence of non-equilibrium singular points may produce a diverse range of dynamics.

Table 1. Stabilities of singular points. Abbreviations are defined as follows. WH: N-unstable & J-stable parts; BL: N-unstable & J-unstable parts; LG : N-stable & J-stable parts; and DG: N-stable & J-unstable parts.

	Equilibrium stability	Non-equilibrium stability during the shift
Cusp	Bending type	From BL to DG
Butterfly	Bending type	From BL to DG via WH and LG

Table 2. Stabilities and geometric quantities in KCC theory.

	Stability	Stability change during the shift
N-stability	Non-linear connection N	Berwald connection B
J-stability	Deviation curvature P	Douglas tensor D

Table 3. Types of bifurcation curves and their conditions in KCC theory.

	Equilibrium curve	Non-equilibrium curve
$g = 0, N = 0$	Always	NA
$N = 0, P = 0$	$G_{N_0P_0} \neq 0$	$G_{N_0P_0} = 0$

Table 4. Singular points in equilibrium and non-equilibrium curves considered in this paper.

	Equilibrium singular points	Non-equilibrium singular points
Cusp	Cusp	NA
Swallowtail	Swallowtail, Cusp	Cusp
Butterfly	Butterfly, Cusp	Swallowtail, Cusp

References

Abolghasem, H. [2013b] "Jacobi stability of hamiltonian systems," *Int. J. Pure Appl. Math.* **87**, 181–194.

Antonelli, P., Rutz, S., & Strychar, K. B. "Heat stress on scleractinian corals: Its symbionts in evolution," *Nonlinear Anal. RWA.* **28**, 189-196.

Antonelli, P.L. [1985] *Mathematical Essays on Growth and the Emergence of Form*, (University of Alberta Press, Alberta).

Antonelli, P.L., Ingarden, R.S. & Matsumoto, M. [1993] *The Theory of Sprays and Finsler Spaces with Applications in Physics and Biology*, (Kluwer, Dordrecht).

Antonelli, P. L., & Bucataru, I. [2001] "New results about the geometric invariants in KCC-theory," *An. St. Univ. "Al. I. Cuza" Iasi* **47**, 405–420.

Antonelli,, P.L. & Bucataru, I. [2003] *KCC Theory of a System of Second Order Differential Equations, in: Handbook of Finsler Geometry*, (Kluwer, Dordrecht).

Antonelli, P.L., Leandro, E.S. & Rutz, S.F. [2014] "Gradient-driven dynamics on Finsler manifolds: the Jacobi action-metric theorem and an application in ecology," *Nonlinear Stud.* **21**, 141–152.

Antonelli, P. L., Rutz, S. F. & Ferreira Jr, G.S. [2019] "Remarks on modeling serial endosymbiosis and evolution of eukaryote tissue formation," *Nonlinear Stud.* **26**, 653–662.

Antonelli, P.L., Rutz, S.F., & Sabău, S.V. [2002] "A transient-state analysis of Tysonfs model for the cell division cycle by means of KCC-theory," *Open Syst. Inf. Dyn.* **9**, 222–238.

Alawadi, M. A., Batic, D. & Nowakowski, M. [2020] "Light bending in a two black hole metric," *Class. Quantum Grav.* **38**, 045003.

Arnol'd, V. I. [2003] *Catastrophe Theory* (3rd), (Springer Science & Business Media).

Balan, V. & Neagu, M. [2010] "Jet geometrical extension of the KCC-invariants," *Balkan J. Geom. Appl.* **15**, 8–16.

Boehmer, C.G. & Harko, T. [2010] "Nonlinear stability analysis of the emden-fowler equation," *J. Nonlinera. Math. Phy.* **17**, 503–516.

Bröcker, T., & Lander, L. [1975] *Differentiable Germs and Catastrophes*, (Lect. Note Series, 17, London Math. Soc.).

Cartan, E. [1933] "Observations sur le mémoire précédent," *Math. Z.* **37**, 619–622.

Chern, S.S. [1939] "Sur la géométrie d'un systéme d'équations différentielles du second ordre," *Bull. Sci. Math.* **63**, 206–212.

Chen, Y. & Yin, Z. [2019] "The Jacobi stability of a Lorenz-type multistable hyperchaotic system with a curve of equilibria," *Int. J. Bifurcat. Chaos* **29**, 1950062.

Chen, B., Liu, Y., Wei, Z. & Feng, C. [2020] "New insights into a chaotic system with only a Lyapunov stable equilibrium," *Math. Methods Appl. Sci.* **43**, 9262–9279.

Douglas, J. [1927] "The general geometry of paths," *Ann. Math.* **29**, 143–168.

Dănilă, B., Harko, T., Mak, M.K., Pantaragphong, P. & Sabău, S.V. [2016] "Jacobi stability analysis of scalar field models with minimal coupling to gravity in a cosmological background," *Adv. High Ene. Phy.* **2016**, p. 26.

Feng, C., Huang, Q., & Liu, Y. [2020] "Jacobi analysis for an unusual 3D autonomous system," *Int. J. Geom. Methods Mod. Phys.* **17**, 2050062.

Fujimori, S., Saji, K., Umehara, M., & Yamada, K. [2008] "Singularities of maximal surfaces," *Math. Z.* **259**, 827.

Gilmore, R. [1981] *Catastrophe Theory for Scientists and Engineers*, (Dover, New York).

Gupta, M. K., & Yadav, C. K. [2017] "Jacobi stability analysis of Rössler system," *Int. J. Bifurcat. Chaos*, **27**, 1750056.

Gupta, M. K., & Yadav, C. K. [2017] "Jacobi stability analysis of modified Chua circuit system," *Int. J. Geom. Methods Mod. Phys.* **14**, 1750089.

Gupta, M. K. & Yadav, C. K. [2019] "Rabinovich-Fabrikant system in view point of KCC theory in Finsler geometry," *J. Interdiscip. Math.* **22**, 219–241.

Hutchinson G.E. [1948] "Circular causal systems in ecology," *Ann. NY Acad. Sci.* **50**, 221–246.

Harko, T. & Sabău, S.V. [2008] "Jacobi stability of the vacuum in the static spherically symmetric brane world models," *Phys. Rev. D.* **77**, 104009.

Harko, T., Ho, C.Y., Leung, C.S. & Yip, S. [2015] "Jacobi stability analysis of the Lorenz system," *Int. J. Geo. Meth. Mod. Phy.* **12**, 1550081.

Harko, T., Pantaragphong, P. & Sabău, S.V. [2016] "Kosambi-Cartan-Chern (KCC) theory for higher-order dynamical systems," *Int. J. Geo. Meth. Mod. Phy.* **13**, 1650014.

Hasegawa, M., Honda, A., Naokawa, K., Saji, K., Umehara, M., & Yamada, K. [2015] "Intrinsic properties of surfaces with singularities," *Intarnat. J. Math.* **26**, 1540008.

Huang, Q., Liu, A. & Liu, Y. [2019] "Jacobi stability analysis of the Chen system," *Int. J. Bifurcat. Chaos* **29**, 1950139.

Izumiya, S., & Saji, K. [2010] "The mandala of Legendrian dualities for pseudo-spheres in Lorentz-Minkowski space and "flat" spacelike surfaces," *J. Singul.* **2**, 92–127.

Izumiya, S., Saji, K., & Takahashi, M. [2010] "Horospherical flat surfaces in hyperbolic 3-space," *Japanese J. Math.* **62**, 789–849.

Izumiya, S., Romero Fuster, M. D. C., Ruas, M. A. S., & Tari, F. [2016] *Differential Geometry from a Singularity Theory Viewpoint*, (World Scientific).

Klën, W. S. & Molina, C. [2020] "Dynamical analysis of null geodesics in brane-world spacetimes," *Phys. Rev. D* **102**, 104051.

Kokubu, K., Rossman, W., Saji, K., Umehara U., & Yamada, K. [2005] "Singularities of flat fronts in hyperbolic 3-space," *Pacific J. Math.* **221**, 303 – 351.

Kolebaje, O. & Popoola, O. [2019] "Jacobi stability analysis of predator-prey models with holling-type II and III functional responses," *AIP Conf. Proc.* **2184**, 060001.

Kosambi D.D. [1933] "Parallelism and path-spaces," *Math. Z.* **37**, 608–618.

Krylova, N., Voynova, Y. & Balan, V. [2019] "Application of geometrical methods to study the systems of differential equations for quantum-mechanical problems," *J. Phys. Conf. Ser.* **1416**, 012021.

Kumar, M., Mishra, T. N. & Tiwari, B. [2019] "Stability analysis of Navier-Stokes system," *Int. J. Geom. Methods Mod. Phys.* **16**, 1950157.

Lake, M.J. & Harko, T. [2016] "Dynamical behavior and Jacobi stability analysis of wound strings," *Eur. Phys. J.* **76**, 1–26.

Liu, A., Chen, B. & Wei, Y. [2020] "Jacobi analysis of a segmented disc dynamo system," *Int. J. Geom. Methods Mod. Phys.* **17**, 2050205.

Liu, Y., Huang, Q. & Wei, Z. [2021] "Dynamics at infinity and Jacobi stability of trajectories for the Yang-Chen system," *Discrete. Contin. Dyn. Syst. Ser. B* **26**, 3357-3380.

Liu, Y., Li, C., & Liu, A. [2021] "Analysis of geometric invariants for three types of bifurcations in 2D differential systems," *Int. J. Bifurcat. Chaos* **31**, 2150105.

Ludwig, D., Jones, D. D., & Holling, C. S. [1978] "Qualitative analysis of insect outbreak systems: the spruce budworm and forest," *J. Anim. Ecol.* **47**, 315–332.

Martins L.F., & Saji, K. [2016] "Geometric invariants of cuspidal edges," *Canad. J. Math.* **68**, 445–462.

Martins, L.F., Saji, K., Umehara M., & Yamada, K. [2016] "Behavior of Gaussian curvature and mean curvature near non-degenerate singular points on wave fronts," *Geometry and Topology of Manifolds* (Springer, Tokyo), 247–281

Mishra, T. N., & Tiwari, B. [2021] "Stability and bifurcation analysis of a prey-predator model," *Int. J. Bifurcat. Chaos* **31**, 2150059.

Mori, A. S. [2011] "Ecosystem management based on natural disturbances: hierarchical context and non-equilibrium paradigm," *J. Appl. Ecol.* **48**, 280–292.

Neagu, M. [2013] "Multi-time Kosambi-Cartan-Chern invariants and applications," *BSG Proceedings.* **20**, 36–50.

Pickett, S. T. [1980] "Non-equilibrium coexistence of plants," *Bull. Torrey Bot. Club*, **107**, 238–248.

Porteous, I.R., [2001] *Geometric differentiation. For the intelligence of curves and surfaces* (2nd edition), (Cambridge University Press, Cambridge).

Poston, T., & Stewart, I. [1978] *Catastrophe Theory and its Applications* (Pitman Publishing Limited, London).

Raup, D., & Stanley, S. M. [1978] *Principles of Paleontology*, (W.H. Freeman, San Francisco).

Sabău, S.V. [2005a] "Some remarks on Jacobi stability," *Nonlinear Anal. TMA.* **63**, e143–e153.

Sabău, S.V. [2005b] "Systems biology and deviation curvature tensor," *Nonlinear Anal. RWA.* **6**, 563–587.

Saji, K., Umehara M., & Yamada, K., [2009] "The geometry of fronts," *Ann. of Math.* **169**, 491 – -529.

Saji, K., Umehara M., & Yamada, K., [2010] "The duality between singular points and inflection points on wave fronts," *Osaka J. Math.* **47** 591–607.

Saji, K., & Teramoto, K. [2020] "Dualities of differential geometric invariants on cuspidal edges on flat fronts in the hyperbolic space and the de Sitter space," *Mediterr. J. Math.* **17**, 1–20.

Salnikova, T. V., Kugushev, E. I. & Stepanov, S. Y. [2020] "Jacobi stability of a many-body system with modified potential," *Doklady Mathematics* **101**, 154–157.

Scheffer, M., Bascompte, J., Brock, W. A., Brovkin, V., Carpenter, S. R., Dakos, V., Held H., Van Nes, E.H., Rietkerk, M., & Sugihara, G. [2009] "Early-warning signals for critical transitions," *Nature* **461**, 53.

Shiba, S., & Umehara, M. [2012] "The behavior of curvature functions at cusps and inflection points,"

Differential Geom. Appl. **30**, 285–299.
Strogatz, S.H. [2014] *Nonlinear Dynamics and Chaos: with Applications to Physics, Biology, Chemistry, and Engineering*, (Westview press, USA).
Sprugel, D. G. [1991] "Disturbance, equilibrium, and environmental variability: what is 'natural' vegetation in a changing environment?," *Biol. Conserv.* **58**, 1–18.
Sulimov, V. D., Shkapov, P. M. & Sulimov, A. V. [2018] "Jacobi stability and updating parameters of dynamical systems using hybrid algorithms," *IOP Conf. Ser. Mater. Sci. Eng.* **468**, 012040.
Thom, R. [1972] *Stabilité Structurelle et Morphogénèse*, (Benjamin, New York).
Thompson, J.M.T. [1982] *Instabilities and Catastrophes in Science and Engineering* (John Willy & Sons, New York).
Udrişte, C. & Nicola, I.R. [2009] "Jacobi stability of linearized geometric dynamics," *J. Dyn. Syst. Geom. Theor.* **7**, 161–173.
Umehara, M. [2011] "A simplification of the proof of Bol's conjecture on sextactic points," *P. JPN Acad. A-Math.* **87**, 10–12.
Wang, F., Liu, T., Kuznetsov, N. V., & Wei, Z. [2021] "Jacobi stability analysis and the onset of chaos in a two-degree-of-freedom Mechanical System," *Int. J. Bifurcat. Chaos* **31**, 2150075.
Wright, E. M. [1955] "A non-linear difference-differential equation," *J. Reine Angew. Math*, **194**, 66–87.
Yajima, T., Yamasaki, K., & Nagahama, H. [2018] "Non-holonomic geometric structures of rigid body system in Riemann-Cartan space," *J. Phys. Commun.* **2**, 085008.
Yamasaki, K. & Yajima, T. [2013] "Lotka-Volterra system and KCC theory: Differential geometric structure of competitions and predations," *Nonlinear Anal. RWA.* **14**, 1845–1853.
Yamasaki, K. & Yajima, T. [2016] "Differential geometric structure of non-equilibrium dynamics in competition and predation: Finsler geometry and KCC theory," *J. Dyn. Syst. Geom. Theor.* **14**, 137–153.
Yamasaki, K. & Yajima, T. [2017] "KCC analysis of the normal form of typical bifurcations in one-dimensional dynamical systems: Geometrical invariants of saddle-node, transcritical, and pitchfork bifurcations," *Int. J. Bifurcat. Chaos*, **27**, 1750145.
Yamasaki, K. & Yajima, T. [2020] "KCC Analysis of a one-dimensional system during catastrophic shift of the Hill function: Douglas tensor in the nonequilibrium region," *Int. J. Bifurcat. Chaos*, **30**, 2030032.
Zeeman, E.C. [1977], *Catastrophe Theory: Selected Papers 1972-1977* (Addison-Wesley, Boston).